

Universal flow-density relation of single-file bicycle, pedestrian and car motion

J. Zhang, W. Mehner, S. Holl, and M. Boltes

*Jülich Supercomputing Centre, Forschungszentrum Jülich GmbH, 52425 Jülich, Germany**

E. Andresen

*Department of Computer Simulation for Fire Safety and Pedestrian Traffic,
Bergische Universität Wuppertal, 42285 Wuppertal, Germany†*

A. Schadschneider

Institut für Theoretische Physik, Universität zu Köln, 50937 Köln, Germany‡

A. Seyfried

*Jülich Supercomputing Centre, Forschungszentrum Jülich GmbH, 52425 Jülich, Germany and
Department of Computer Simulation for Fire Safety and Pedestrian Traffic,
Bergische Universität Wuppertal, 42285 Wuppertal, Germany§*

The relation between flow and density is an essential quantitative characteristic to describe the efficiency of traffic systems. We have performed experiments with single-file motion of bicycles and compare the results with previous studies for car and pedestrian motion in similar setups. In the space-time diagrams we observe three different states of motion (free flow state, jammed state and stop-and-go waves) in all these systems. Despite of their obvious differences they are described by a universal fundamental diagram after proper rescaling of space and time which takes into account the size and free velocity of the three kinds of agents. This indicates that the similarities between the systems go deeper than expected.

PACS numbers: 45.70.Vn, 05.60.-k, 89.40.Bb, 89.75.Fb, 02.50.Ey

INTRODUCTION

In the past, various studies have been performed on pedestrian [1], bicycle [2] and vehicular traffic [3–6]. Besides the obvious practical relevance, from a physics point-of-view, these traffic systems are interesting for the observed collective and self-organization phenomena, phase transitions etc. Most of the methods and theories in pedestrian dynamics are borrowed from vehicular traffic. As for the study of bicycle traffic, most research focuses on operating characteristics, travel speed distributions as well as bicycle characteristics. Only a small number of studies focused on the flow properties of bicycle traffic [7–10]. Here we want to find out how strongly the flow-density relation depends on the properties of the agents.

Usually these different types of traffic flows are investigated separately. So far a systematic comparison has not been attempted but qualitative similarities are obvious. Nearly all studies on pedestrians and vehicles show that the speed decreases with the density. At a certain critical value of the density the flow is unstable and transits from free flow to jammed flow. This transition was also found for bicycle flows [10]. In this work single-file pedestrian, car and bicycle movement on a planar circuit will be studied under laboratory conditions. We analyze, on a quantitative level, similarities and differences between the flow-density relation of these three traffic modes. We want to study whether they can be derived from a uni-

versal flow-density relation.

EXPERIMENTAL SETUP

The experiments for all three types of traffic were performed with similar setups, namely on planar circuits where only single-file motion was possible. Series of experiments were carried out with a maximal number of participants $N = 70$, 23 and 33 for the pedestrian, car and bicycle experiment, respectively. In general, participants were asked to move normally without overtaking. The global density was varied by repeating the experiment with different numbers of participants.

The pedestrian experiment [11] was performed with soldiers moving in a circular corridor of circumference $C_p = 26$ m. During the experiment the soldiers were asked to walk in a normal fashion but not in lockstep (see the video from [12]). The one dimensional global density $\rho_g = N/C$ ranges from 0.54 m^{-1} to 2.69 m^{-1} in this experiment.

A similar experiment with cars was performed by Sugiyama et al. [13, 14] on a circular road with circumference $C_c = 230$ m and $N = 22$ and 23, corresponding to global densities $\rho_g = 0.096 \text{ m}^{-1}$ and 0.1 m^{-1} , respectively. Recently the same group improved these experiments [15]. They carried out 19 experimental runs with $C_c = 312$ m and different numbers of cars (N was changed from 10 to 40). The global density ρ_g in this



FIG. 1. Snapshots of the bicycle experiment on a circuit road.

experiment ranges from 0.03 m^{-1} to 0.13 m^{-1} .

The bicycle experiment was carried out in Germany in 2012 with participants of all ages [16]. On a circuit road with circumference $C_b = 86 \text{ m}$ several runs with different numbers of bicycles (from $N = 5$ to $N = 33$) were performed (Fig. 1). Based on video recordings [17] the trajectories were extracted automatically, similar to the method used in the pedestrian experiments [18]. Details will be given elsewhere [16].

TRAJECTORIES

From the high precision trajectories, traffic flow characteristics including flow, density and velocity can be determined. Fig. 2 shows a time-space diagram in the measurement area, which has a length of 27 m , from one run of the bicycle experiment. Similar trajectory plots for car and pedestrian motion can be found in [11, 13].

In all three cases a transition from free flow to jammed flow can be observed with the increasing of the global density. In the free flow regime all agents can move at their desired speed, whereas in the jammed regime typically stop-and-go waves are observed.

METHODS OF DATA ANALYSIS

The comparison of time-space diagrams already indicates a qualitative similarity between the three traffic systems. A deeper understanding requires quantitative analysis which allows to uncover the underlying dynamics that is not apparent in the more qualitative observa-

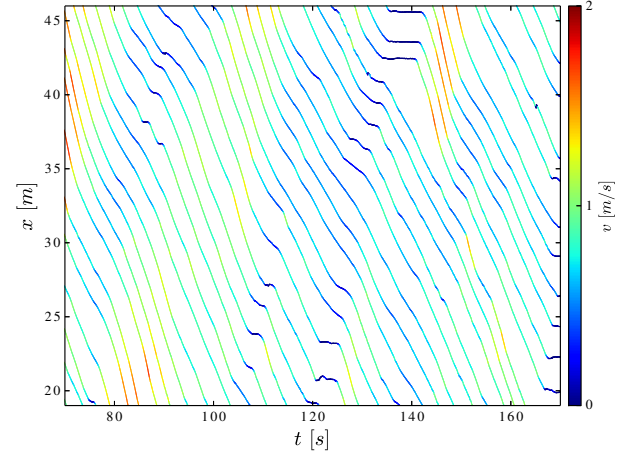


FIG. 2. Trajectories in the measurement area (of length 27 m) for the bicycle experiment with $N = 33$. The same structures can be found in trajectories of pedestrian and vehicle systems [11, 13].

tions of the trajectories. We use both macroscopic and microscopic analysis to obtain more detailed information on the specific flow-density relation or equivalently the velocity-density relation. In this study the specific flow J_s is calculated by $J_s = \rho \cdot v$.

Microscopically, an individual density can either be defined based on a Voronoi tessellation [19] or the headway. The headway $d_H(i)$ is defined as the distance between the centers of mass of an agent i and its predecessor, whereas the Voronoi space $d_V(i)$, for one-dimensional motion, is the distance between the midpoints of the headway and the headway of its follower $i - 1$. The corresponding individual densities are then $\rho_H(i) = 1/d_H(i)$ and $\rho_V(i) = 1/d_V(i)$, respectively. As for the individual velocity, the instantaneous velocity $v_i(t)$ is defined as

$$v_i(t) = \frac{x_i(t + \Delta t'/2) - x_i(t - \Delta t'/2)}{\Delta t'}, \quad (1)$$

where $x_i(t)$ is the x coordinate of pedestrian i at time t and $\Delta t' = 2 \text{ s}$ is used in this study.

The individual flow-density relation of bicycle traffic obtained from the Voronoi-based and headway-based methods do not show large discrepancies but the results of the headway-based method are more scattered. This has previously been observed for pedestrian dynamics [19, 20].

Macroscopically, the similarities between the three systems are more apparent. On the macroscopic level the mean densities $\rho(t)$ and velocities $v(t)$ in a measurement area at time t are calculated based on Voronoi method:

$$\rho(t) = \frac{\sum_{i=1}^n \Theta_i(t)}{l_m}, \quad (2)$$

$$v(t) = \frac{\sum_{i=1}^n \Theta_i(t) \cdot v_i(t)}{l_m}, \quad (3)$$

where n is the number of agents whose Voronoi space includes the measurement area (assuming that the overlapping length between the space and the measurement area is $d_o(i)$ for agent i). $\Theta_i(t) = d_o(i)/d_V(i)$ represents the contribution of agent i to the density of the measurement area. $v_i(t)$ is the instantaneous velocity (see eq. (1)) and l_m is the length of the measurement area.

In this study, the lengths of the measurement areas l_m were 3 m, 35 m and 13 m in the pedestrian, car and bicycle experiments, respectively. Since the (average) length of agents is 0.4 m, 3.9 m and 1.73 m, at most 7 agents can occupy the measurement area at the same time. It should be noted that in all experiments the ratio of agent length and system length was of the same order of magnitude.

RESULTS

The flow-density relation of the pedestrian experiment can be divided into three regimes $\rho \in [0, 1.0] \text{ m}^{-1}$, $[1.0, 1.7] \text{ m}^{-1}$ and $[1.7, 3.0] \text{ m}^{-1}$, which correspond to three states of pedestrian movement (see Fig. 3). For small densities $\rho < 1.0 \text{ m}^{-1}$ free flow is observed and the specific flow increases monotonically with the density. A gap can be observed in the velocity-density relationship at $\rho = 1.0 \text{ m}^{-1}$, where a transition occurs in the specific flow-density relationship. When the number of pedestrians inside the system increases from 25 to 28, the specific flow jumps from 1.0 s^{-1} to 0.7 s^{-1} . For $\rho > 1.0 \text{ m}^{-1}$, the stream is in a congested state and the specific flow starts to decrease with the increasing density. However, the decline rates are different around 1.7 m^{-1} . The transient decelerations of pedestrians can be observed sometimes but are not the main property of the movement for $\rho < 1.7 \text{ m}^{-1}$. For $\rho > 1.7 \text{ m}^{-1}$, stop-and-go waves dominate the motion of the pedestrians, which can be seen in [11].

Similar results are observed in the bicycle system, as shown in Fig. 4. For densities $\rho < 0.3 \text{ m}^{-1}$, the bicycle stream is in a free flow state and the specific flow increases monotonically with increasing density. At $\rho = 0.3 \text{ m}^{-1}$ the specific flow drops sharply from 1.0 s^{-1} to 0.4 s^{-1} marking the transition to the congested state. Stop-and-go waves are observed in the run with $N = 33$.

COMPARISON OF THE FLOW-DENSITY RELATIONS

Plotting the flow-density relation of these three systems in one graph shows that the data points occupy different ranges of density and do not seem to be comparable to each other. To take into account the different scales of sizes and velocities of the agents we rescale these quantities. For the length of the agents we use $L_0(c) = 0.4 \text{ m}$ for pedestrians, $L_0(c) = 3.9 \text{ m}$ for cars [15] and the mean

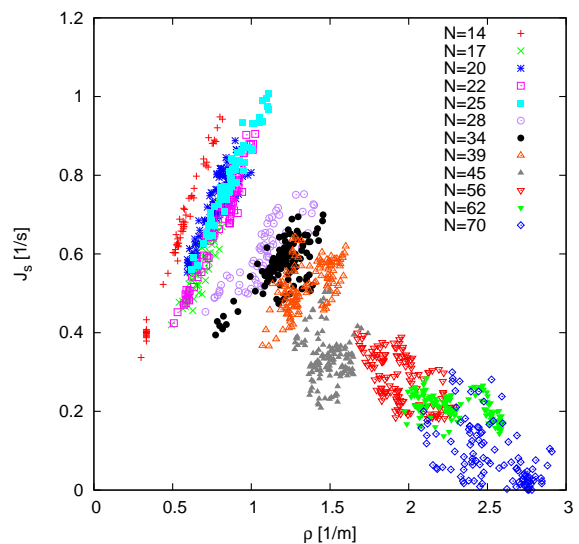


FIG. 3. The Voronoi-based flow-density relation for pedestrians. For $\rho > 1.0 \text{ m}^{-1}$, the free flow regime ends and the specific flow decreases with increasing density.

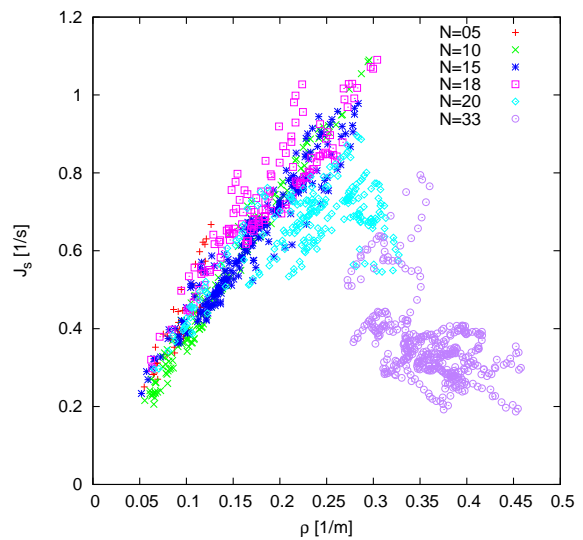


FIG. 4. The Voronoi-based flow-density relation of the bicycle experiment. For $\rho > 0.28 \text{ m}^{-1}$ the free flow regime ends and the flow decreases.

value of $L_0(b) = 1.73 \text{ m}$ of bicycles in the experiment. For scaling the speed we consider the desired velocity of each agent. From special measurements in the course of the experiments we know that they are about 1.4 m/s for pedestrians and 5.5 m/s for bicycles. For cars here we use 11.1 m/s (about 40 km/h) according to the experiment in [15].

After rescaling it is found that the flow-density relations agree well (see Fig. 5). In all cases the free flow regimes ends at approximately $\rho \cdot L_0 = 0.5$. This implies that the transition to the congested state occurs when

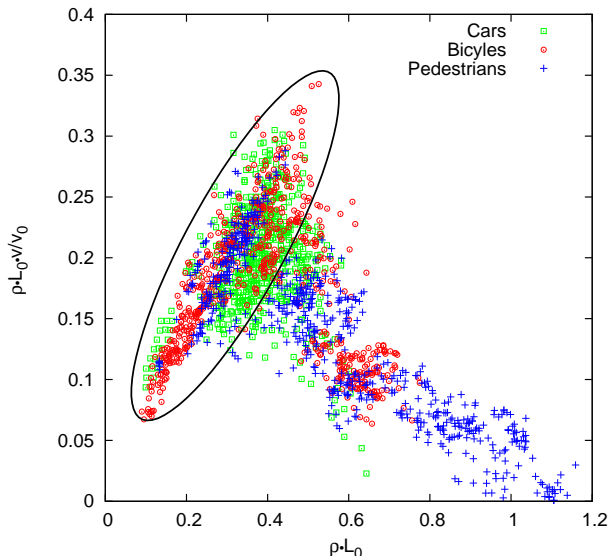


FIG. 5. Comparison of the scaled flow-density relations for pedestrian, car and bicycle traffic. For the scaling the desired velocities (1.4, 11.1 and 5.5 m/s) and agent lengths (0.4, 3.9 and 1.73 m) have been used respectively. The ellipse shows the outline of the free flow regime.

nearly 50% of the available space is occupied. Moreover, the capacity, i.e. the maximal flow, agrees for the three sydiagram are again similar for all three systems. It consists of different states like synchronized traffic and stop-and-go waves. For pedestrians and bicycles, the latter occur at an occupation of 0.7.

Note that the maximum of the scaled densities $\rho \cdot L_0$ is larger than 1.0 for pedestrians. In these experiments no notable body contact was observable and the compressibility of human bodies is not responsible for this effect. Instead pedestrian trajectories are extracted by detecting markers on the head. Head movement in combination with evasion to the side and the projection of the trajectories in one dimension for this comparative analysis is responsible for values of the rescaled density higher than 1. For bicycles, there could be some overlapping of bikes in a zipper-like manner at higher densities which leads to densities larger than 1. In contrast, such overlapping is impossible for car traffic since cars have to keep certain distance to avoid potential collisions. This explains the lack of data for vehicular traffic close to density 1.

DISCUSSION

For single-file systems we showed that the flow-density relations of pedestrian, car and bicycle traffic show a good agreement after simple rescaling. The density at maximal flow and the corresponding flow values are almost identical. This implies that the shape of the flow-density relation does not contain much information about

the type of traffic. This is somewhat unexpected since the traffic systems appear to be governed by rather different aspects. Vehicular traffic is dominated by the physical restrictions on car motion, e.g. inertia effects limiting the possible accelerations. In contrast, in pedestrian motion acceleration and deceleration (and even changes in the direction motion) are almost instantaneous. Bicycle traffic takes an intermediate position between these two extremes.

The transport properties in such systems could be approximated by the universal equation $\tilde{v} = 1 - \tilde{\rho}$ with $\tilde{v} = v/v_0$ and $\tilde{\rho} = \rho/\rho_0$. This leads to a normalized maximal flow of 0.25 at a relative density of 0.5. This corresponds to the properties to the asymmetric simple exclusion process [21, 22], which is often considered as a minimal model for traffic flows. The main feature of this model is volume exclusion. Also models for pedestrian dynamics [23–25] show that these transport characteristics could be reproduced by an appropriate consideration of a velocity dependent volume exclusion, which seems a universal characteristics of such systems. From this we conclude that other properties of the agent, like acceleration or inertia are less relevant for the structure of the flow-density relation in single-file traffic systems of different agent types. In other words models without a proper consideration of the volume exclusion miss an important aspect of traffic systems.

Two exceptions from these observations deserve to be mentioned. First of all, in highway traffic two different congested phases can be distinguished, the wide jam phase and the synchronized phase [5]. The structure of synchronized traffic leads to a non-functional form of the flow-density relation with a non-unique flow-density relation.

The second exception, which is more relevant for the present study, concerns traffic on ant trails. As shown in the empirical study [26] no congested phase exists up to the largest observed densities $\rho \approx 0.8$. The average velocity is almost independent of density and the flow-density diagram consists only of a monotonically increasing free-flow branch.

It is not immediately clear what the origin of this different behavior is. As found in [26] ants move in platoons with small headway, but almost identical velocities.

Summarizing, we have shown that the transport properties of these three different types of single-file traffic flows can be unified in a certain range by a simple scaling of velocity and density. These results may not only provide insights into dynamical behavior but also may be relevant for the improvement of mixed traffic systems. However, to investigate this point further empirical data is still needed especially in the higher density range for bicycle traffic and lower density range for cars.

-
- * ju.zhang@fz-juelich.de; w.mehner@fz-juelich.de;
 † st.holl@fz-juelich.de; m.boltes@fz-juelich.de
 ‡ e.andresen@uni-wuppertal.de
 § as@thp.uni-koeln.de
 § a.seyfried@fz-juelich.de
- [1] A. Schadschneider, W. Klingsch, H. Klüpfel, T. Kretz, C. Rogsch, and A. Seyfried, in *Encyclopedia of Complexity and System Science*, pp. 3142–3176, Springer (2009)
 - [2] D. Taylor and W. J. Davis, *Transp. Res. Rec.* 1974, 102–110 (1999)
 - [3] D. Chowdhury, L. Santen, and A. Schadschneider, *Phys. Rep.* 329, 199–329 (2000)
 - [4] T. Nagatani, *Rep. Prog. Phys.* 65, 1331 (2002)
 - [5] B. S. Kerner, in *The Physics Of Traffic: Empirical Freeway Pattern Features, Engineering Applications, and Theory*, Springer (2004)
 - [6] M. Treiber and A. Kesting, in *Traffic Flow Dynamics*, Springer (2013)
 - [7] D. T. Smith, in *Safety and Locational Criteria for Bicycle Facilities*, Report Federal Highway Administration; No. FHWA-RD-75-112. FHWA, U.S. Department of Transportation (1976)
 - [8] F. P. D. Navin, *ITE Journal* 3, pp. 31–37 (1994)
 - [9] R. Jiang, M. Hu, Q.-S. Wu, W. Song, and B. Wang, Talk given at *Traffic and Granular Flow 11*, 2011.
 - [10] E. Andresen, A. Seyfried, and F. Huber, in *1st SUMO user conference* (2013)
 - [11] A. Seyfried, A. Portz, and A. Schadschneider, *Lecture Notes in Computer Science* 6350, 496–505 (2010)
 - [12] <http://www.asim.uni-wuppertal.de/database-new/own-experiments/corridor/1d-single-file-no-2.html>
 - [13] Y. Sugiyama, M. Fukui, M. Kikuchi, K. Hasebe, A. Nakayama, K. Nishinari, S. Tadaki, and S. Yukawa, *New J. Phys.* 10, 033001 (2008)
 - [14] A. Nakayama, M. Fukui, M. Kikuchi, K. Hasebe, K. Nishinari, Y. Sugiyama, S. Tadaki, and S. Yukawa, *New J. Phys.* 11, 083025 (2009)
 - [15] S. Tadaki, M. Kikuchi, M. Fukui, A. Nakayama, K. Nishinari, A. Shibata, Y. Sugiyama, T. Yosida and S. Yukawa, in *Traffic and Granular Flow 13*, 2013.
 - [16] J. Zhang, W. Mehner, E. Andresen, S. Holl, M. Boltes, A. Schadschneider, and A. Seyfried, in preparation
 - [17] <http://www.asim.uni-wuppertal.de>
 - [18] M. Boltes, A. Seyfried, B. Steffen, and A. Schadschneider, in *Pedestrian and Evacuation Dynamics 2008*, pp. 43–54 (2010)
 - [19] B. Steffen and A. Seyfried, *Physica A* 389, 1902 (2010)
 - [20] J. Zhang, W. Klingsch, A. Schadschneider, and A. Seyfried, *J. Stat. Mech.* (2011) P06004
 - [21] B. Derrida, *Phys. Rep.* 301, 65 (1998)
 - [22] A. Schadschneider, D. Chowdhury, and K. Nishinari, in *Stochastic Transport in Complex Systems: From Molecules to Vehicles*, Elsevier (2010)
 - [23] A. Seyfried, B. Steffen, and T. Lippert, *Physica A* 368, 232–238 (2006)
 - [24] M. Chraïbi, A. Seyfried, and A. Schadschneider, *Phys. Rev. E* 82, 046111 (2010)
 - [25] A. Kirchner, H. Klüpfel, K. Nishinari, A. Schadschneider, and M. Schreckenberg, *J. Stat. Mech.* 10, P10011 (2004)
 - [26] A. John, A. Schadschneider, D. Chowdhury, and K. Nishinari, *Phys. Rev. Lett.* 102, 108001 (2009)